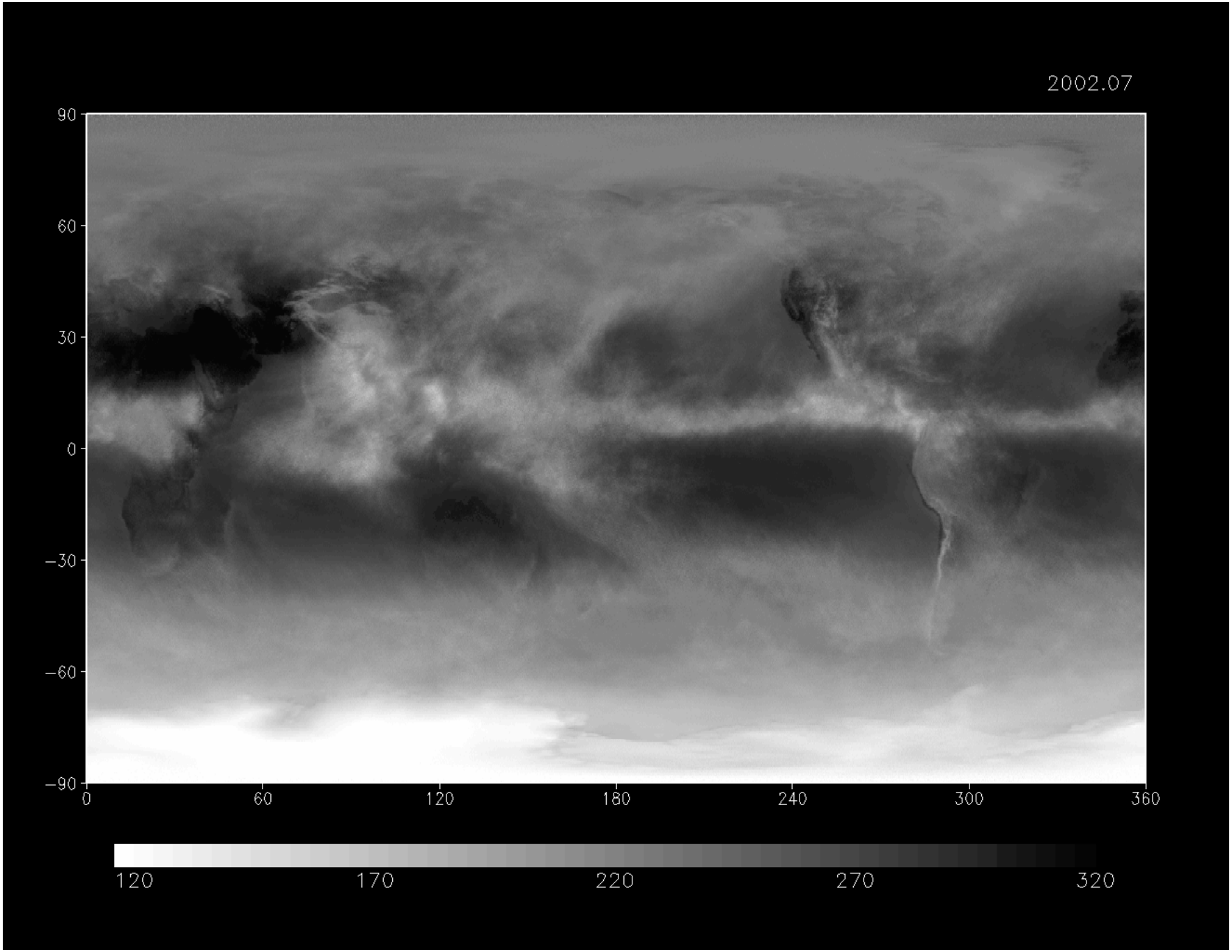
2002.07
90
60
30
0
−30
−60
−90
0
60
120
180
240
300
360
120
170
220
270
320

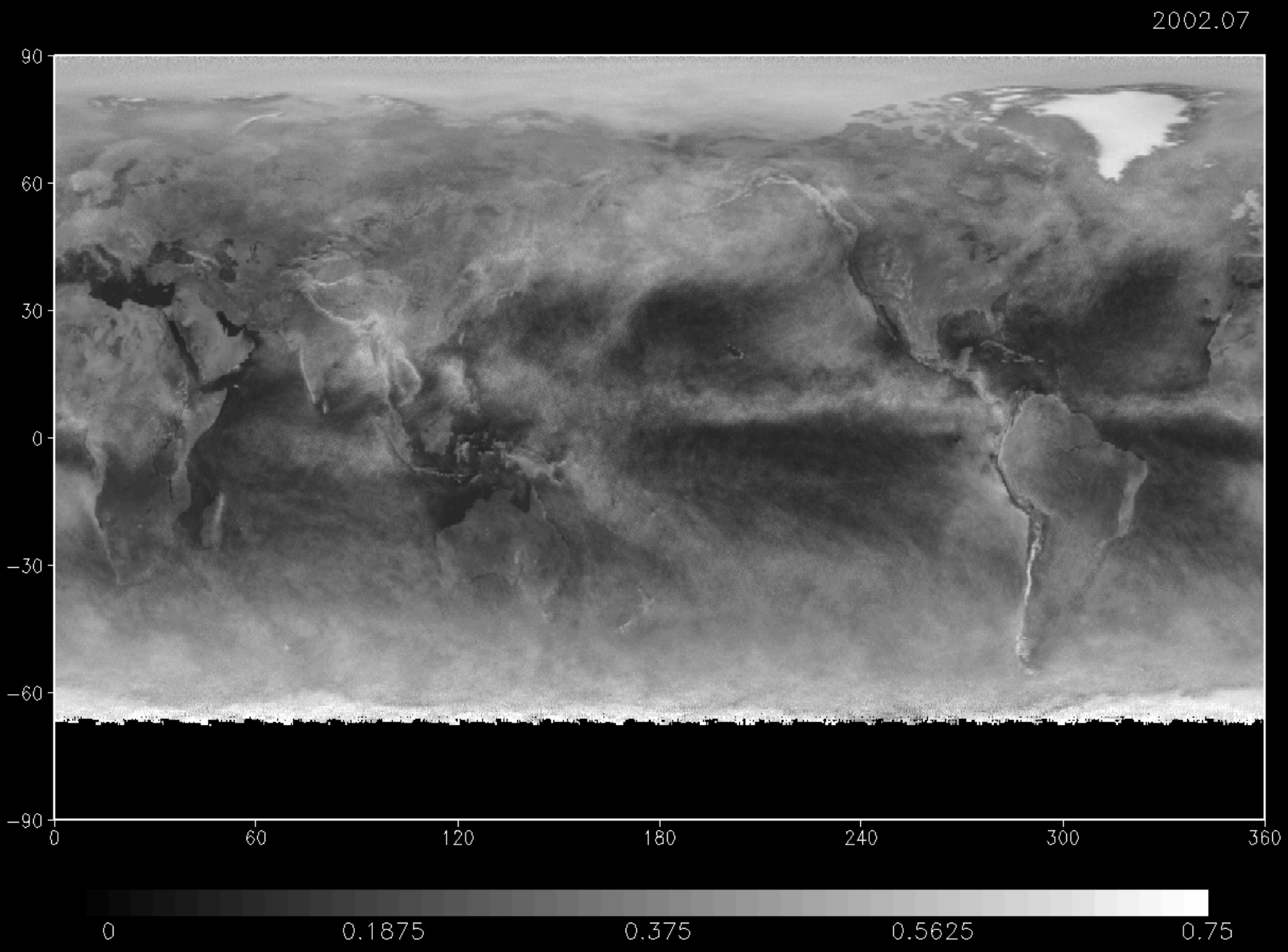
2002.07
90
60
30
0
−30
−60
−90
0
60
120
180
240
300
360
0
0.1875
0.375
0.5625
0.75

Observing Interannual Variations in Hadley Circulation Atmospheric Diabatic Heating and Circulation Strength

Norman G. Loeb[1], David Rutan[2], Seiji Kato[1], Weijie Wang[2,3]

[1]NASA Langley Research Center, Hampton, VA
[2]Science Systems and Applications, Inc., Hampton, VA
[3]Scripps Institute of Oceanography, La Jolla, CA

October 31, 2013, Scripps Institution of Oceanography, La Jolla, CA

Introduction

- Explore use of satellite observations and reanalysis for determining interannual variations in the divergence of dry static and kinetic energy implied by atmospheric diabatic heating within branches of the Hadley Circulation.
- Stratify data according to large-scale domains corresponding to ascending and descending branches of Hadley Circulation.
- How do interannual variations in atmospheric radiation, precipitation, sensible heat and dry static energy divergence co-vary in different circulation regimes?

Data Used

1) Reanalysis

- ERA-Interim monthly meridional wind profiles, surface sensible heat flux, 500 hPa vertical velocity, vertical integral of dry static energy divergence.
- MERRA V5.2: 500 hPa vertical velocity, vertical integral of dry static energy divergence.

2) Satellite

- CERES EBAF Ed2.7 TOA and SFC radiation (March 2000-September 2012).
- GPCP V2.2, TRMM 3A12, TRMM 3B31 precipitation.

Dry Static Energy Budget

- On annual mean time-scale:

$$R_a + LP + S = H$$

R_a = net atmospheric radiation (=$R_{toa} - R_{sfc}$)
P = precipitation rate
L = Latent heat of vaporization
S = Surface sensible heat flux
H = Vertical integral of divergence of dry static and kinetic energy.

$$H = \boldsymbol{\nabla}.\frac{1}{g}\int_0^{p_s}(s+k)\boldsymbol{v}dp$$

where $s=c_p T + gz$ is the dry static energy and k is kinetic energy.

Mass Weighted Zonal Mean Meridional Stream Function (October 2011)

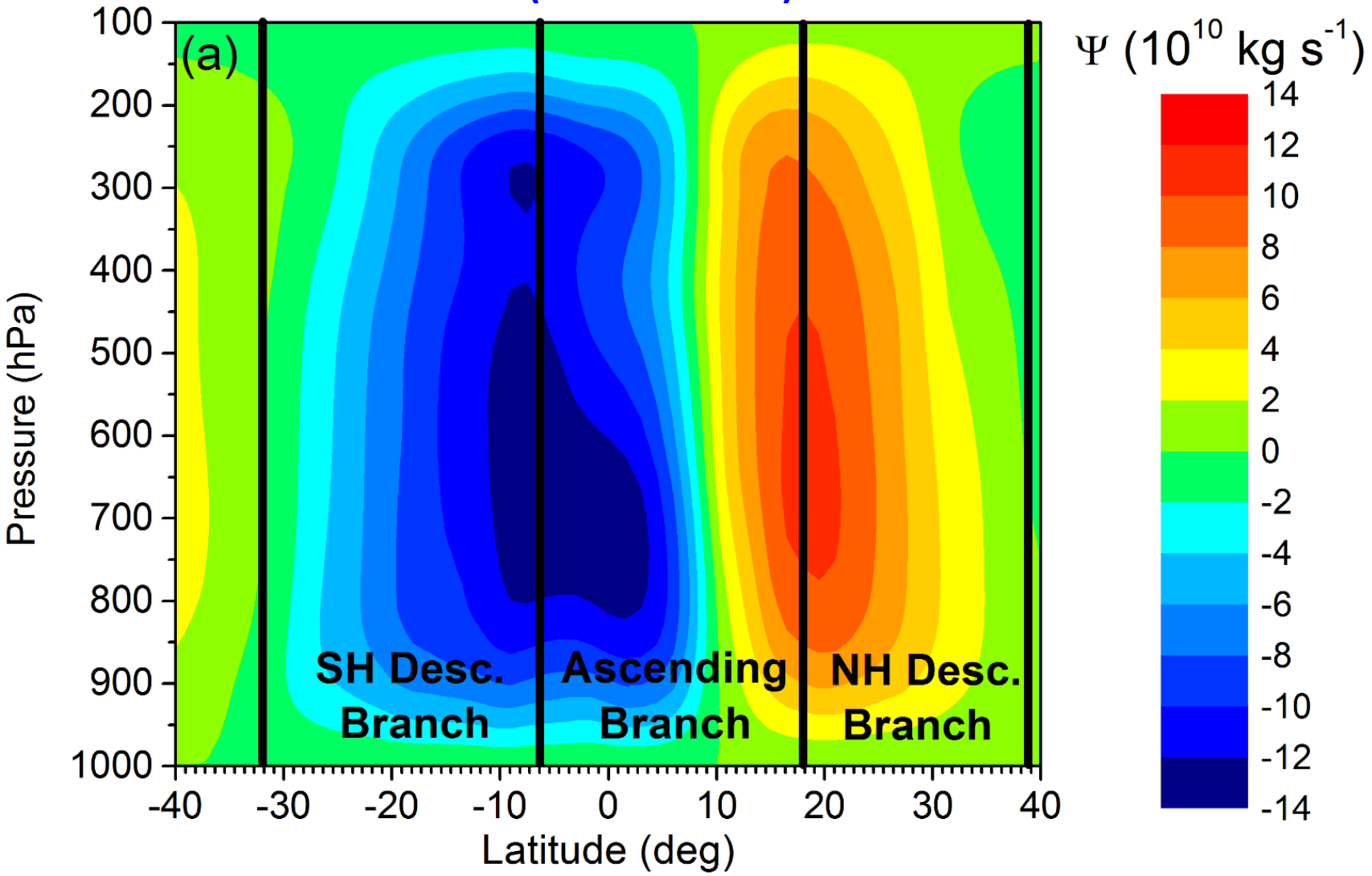

Mean (March 2000-February 2010) TOA LW CRE and SW CRE

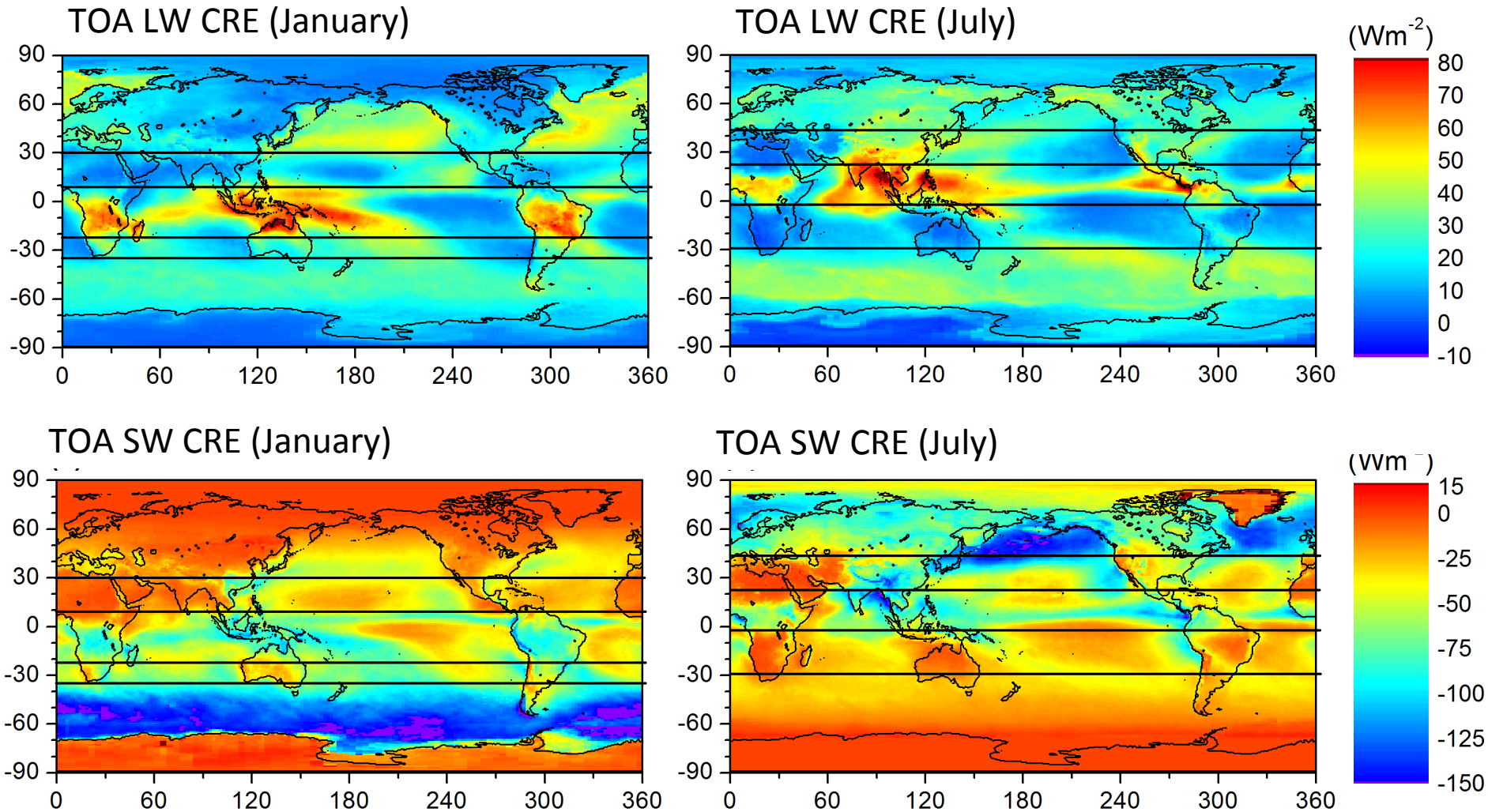

Solid lines show boundaries of ascending and descending branches of the Hadley circulation.

Evaluation of Hadley Circulation Boundaries

Zonal Mean CERES LW CRE for January

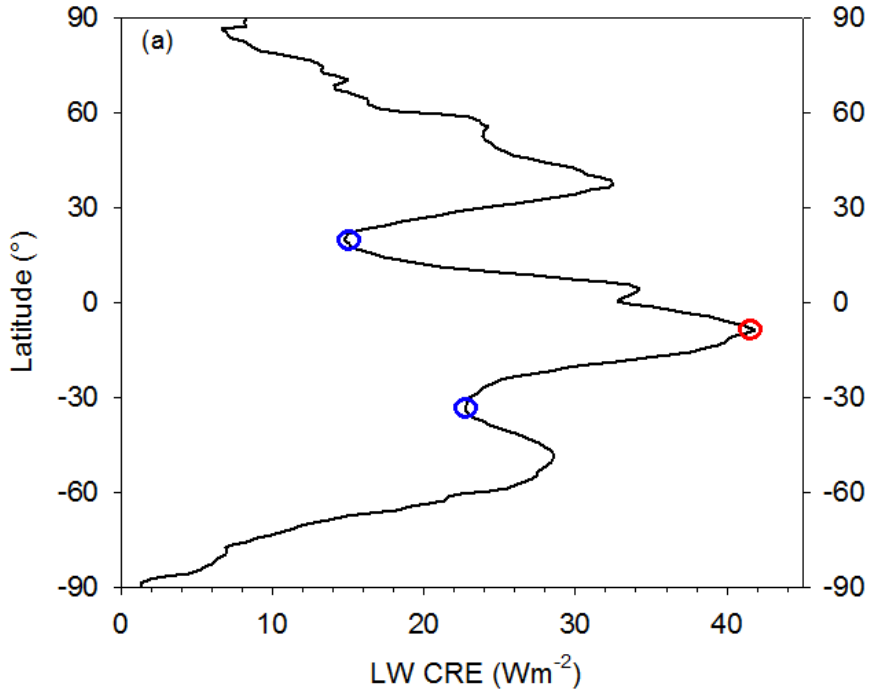

Annual Cycle of HC Boundaries & LW CRE Extrema

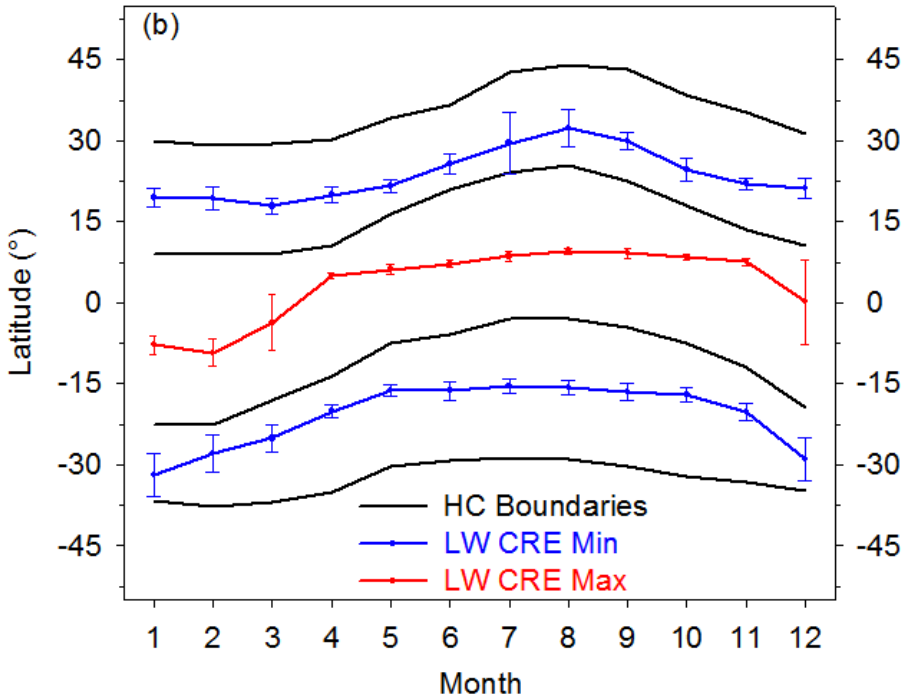

- Minima in LW CRE correspond to the latitude where subsidence reaches a maximum.
- Maximum LW CRE corresponds to the latitude of maximum convection (ITCZ).
- Both track positions of HC boundaries.
- The variability in descending branches is smallest in the wintertime when the HC is strongest (evident from the error bars).

Twelve-month Running Average of Latitudinal Distance Between Positions of NH and SH Subtropical Minima in LW CRE

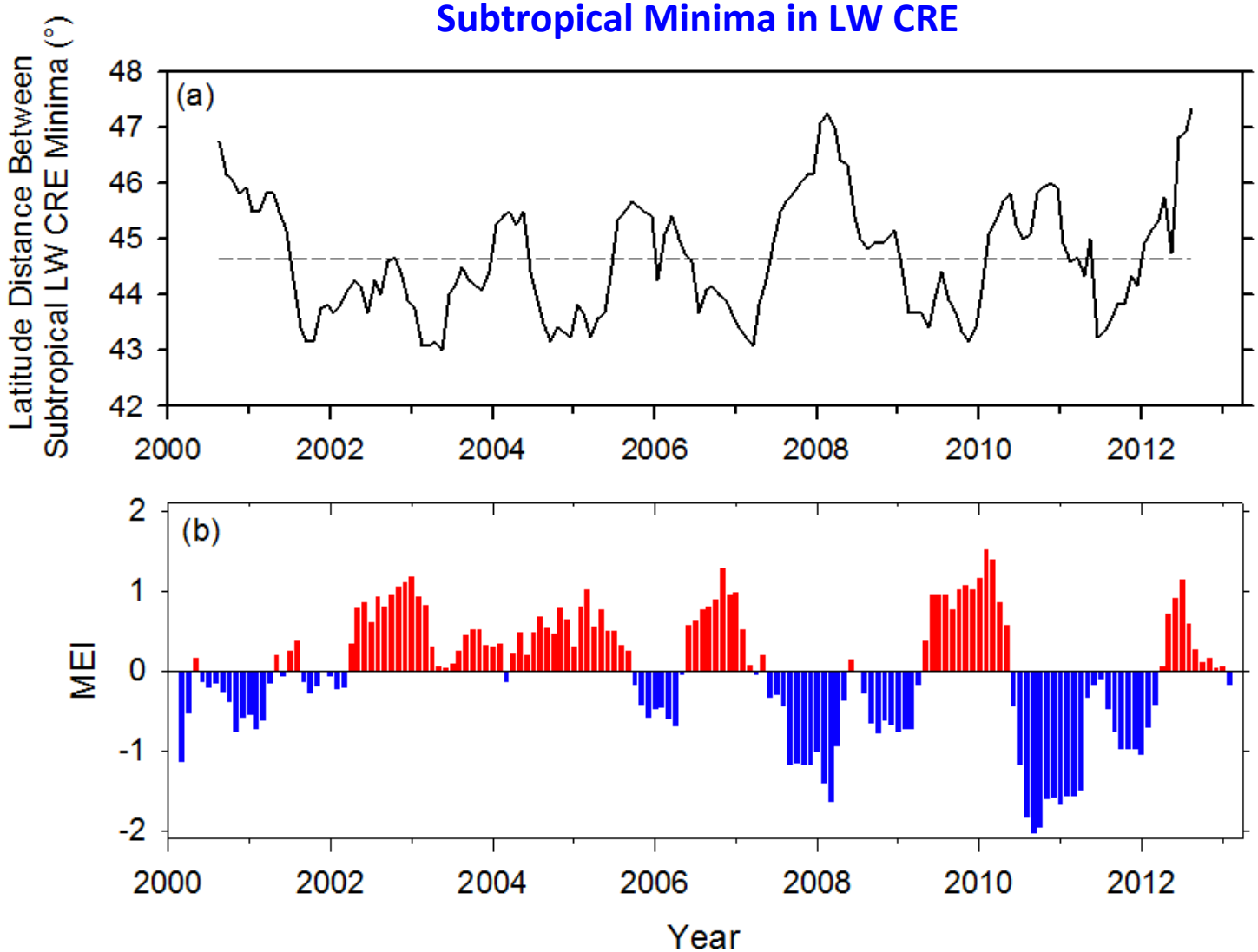

- Width between the positions of NH & SH subtropical maximum subsidence is greater during La Niña (expansion of HC) and smaller (contraction of HC) during El Niño conditions.

Mean of Atmospheric Energy Budget Terms By Longitude (Mar 2000-Feb 2010)

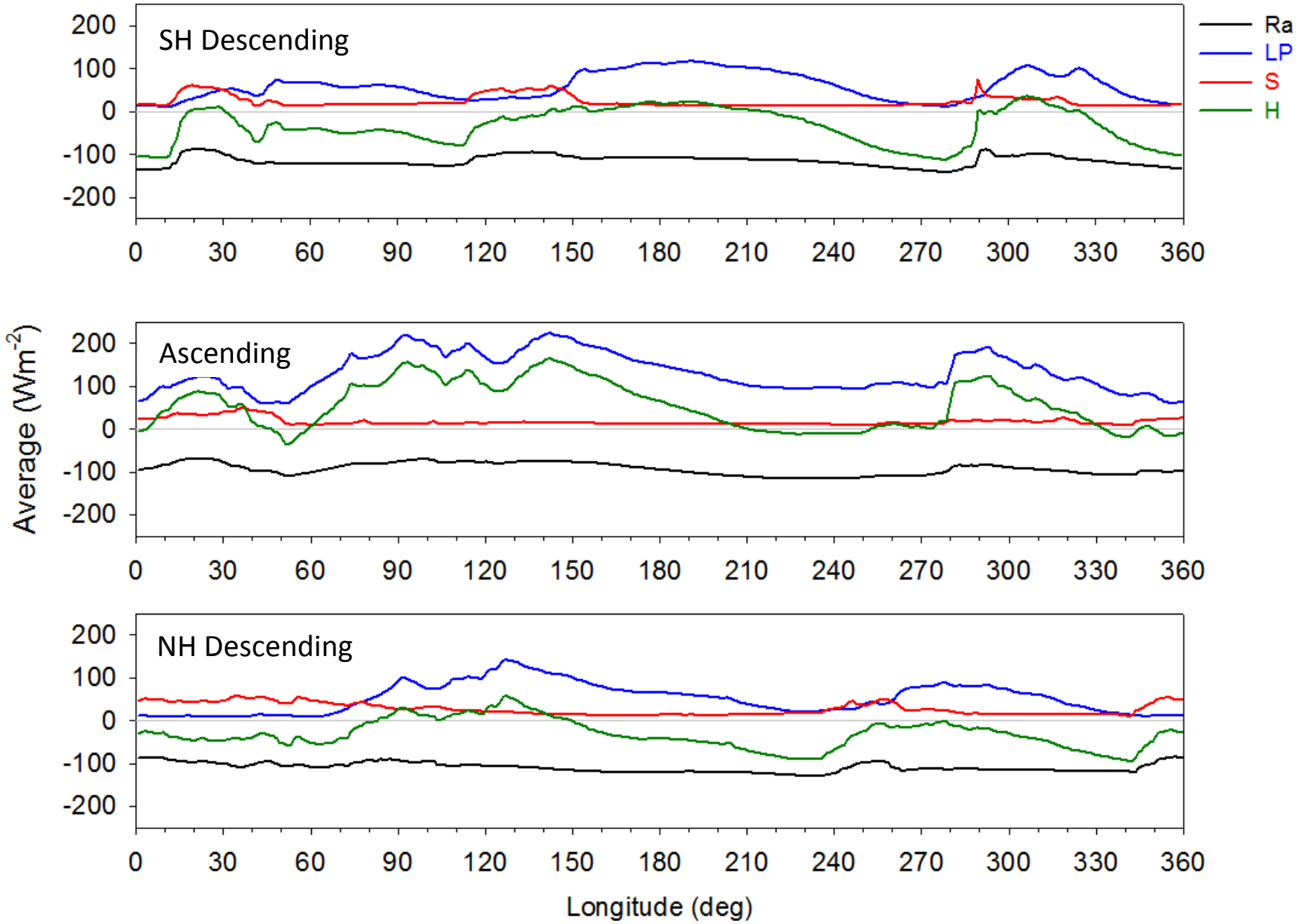

Twelve-month running average of the heat budget terms

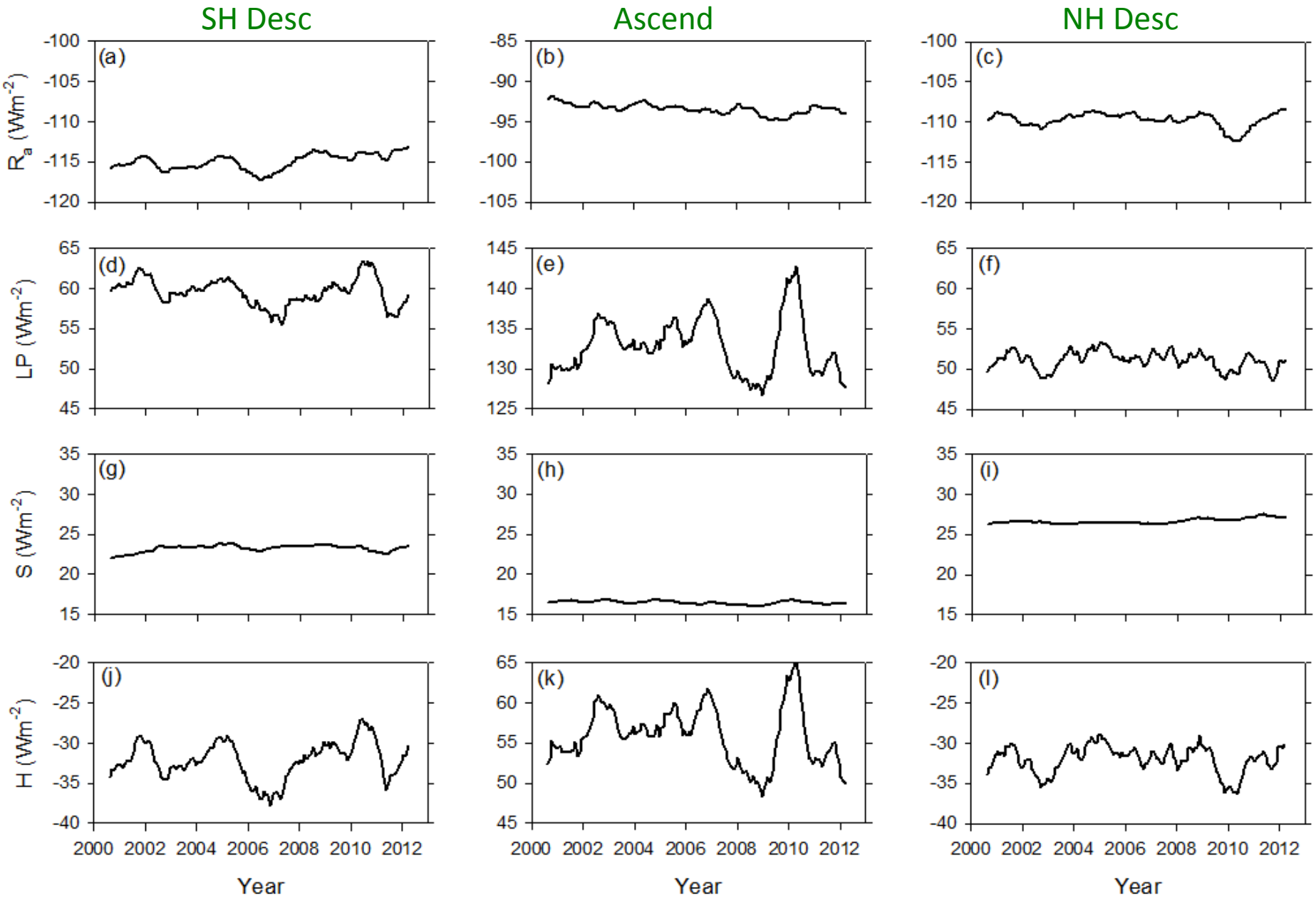

Twelve-month running average of global mean Ra+S and LP, H

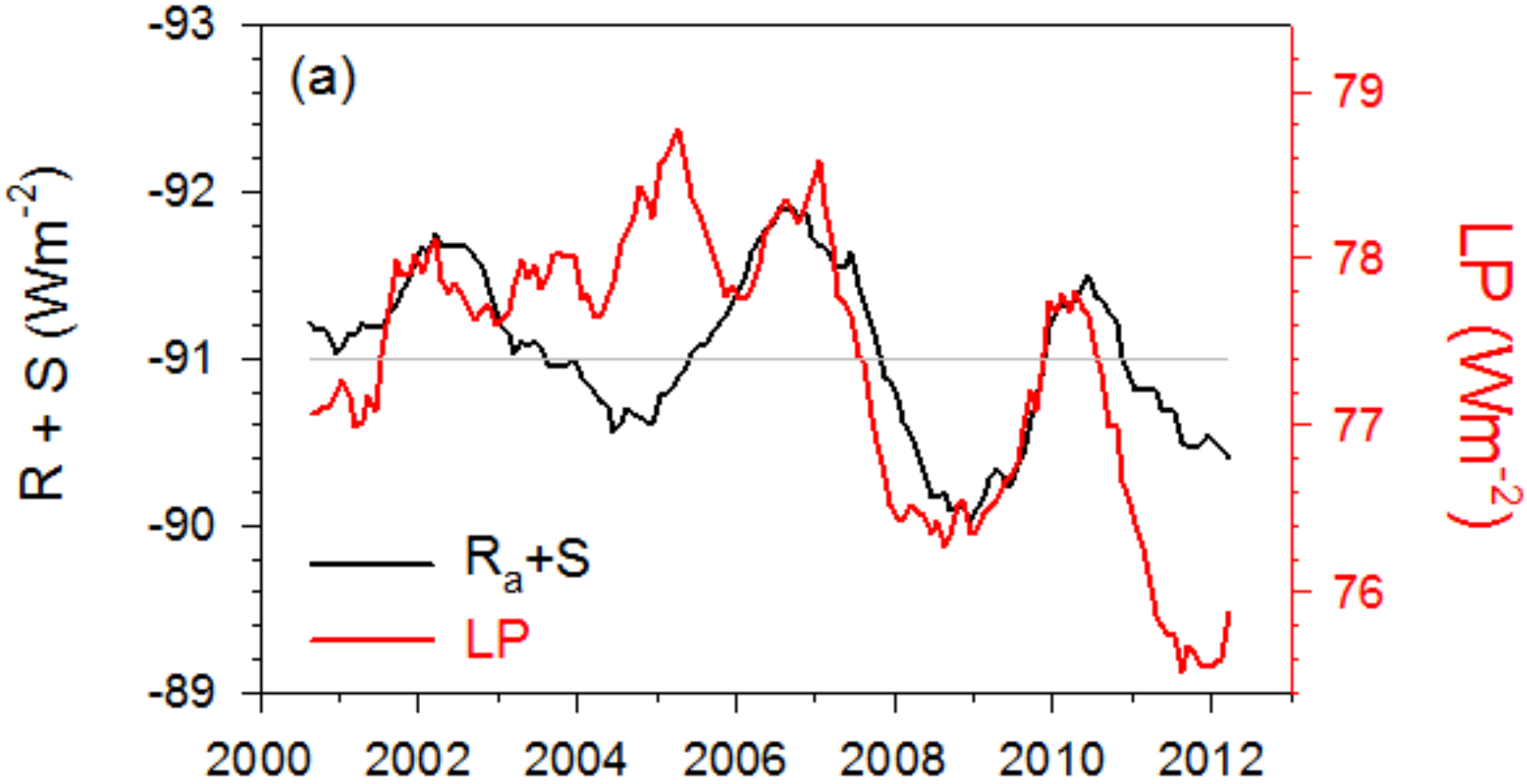

- Despite -14 Wm^{-2} imbalance in global atmospheric energy balance, interannual variations in LP and Ra are consistent.
- Largest discrepancies occur at extrema in LP (2005 and 2012).

GPCP minus TRMM (3A12) LP difference (March 2000-September 2012)

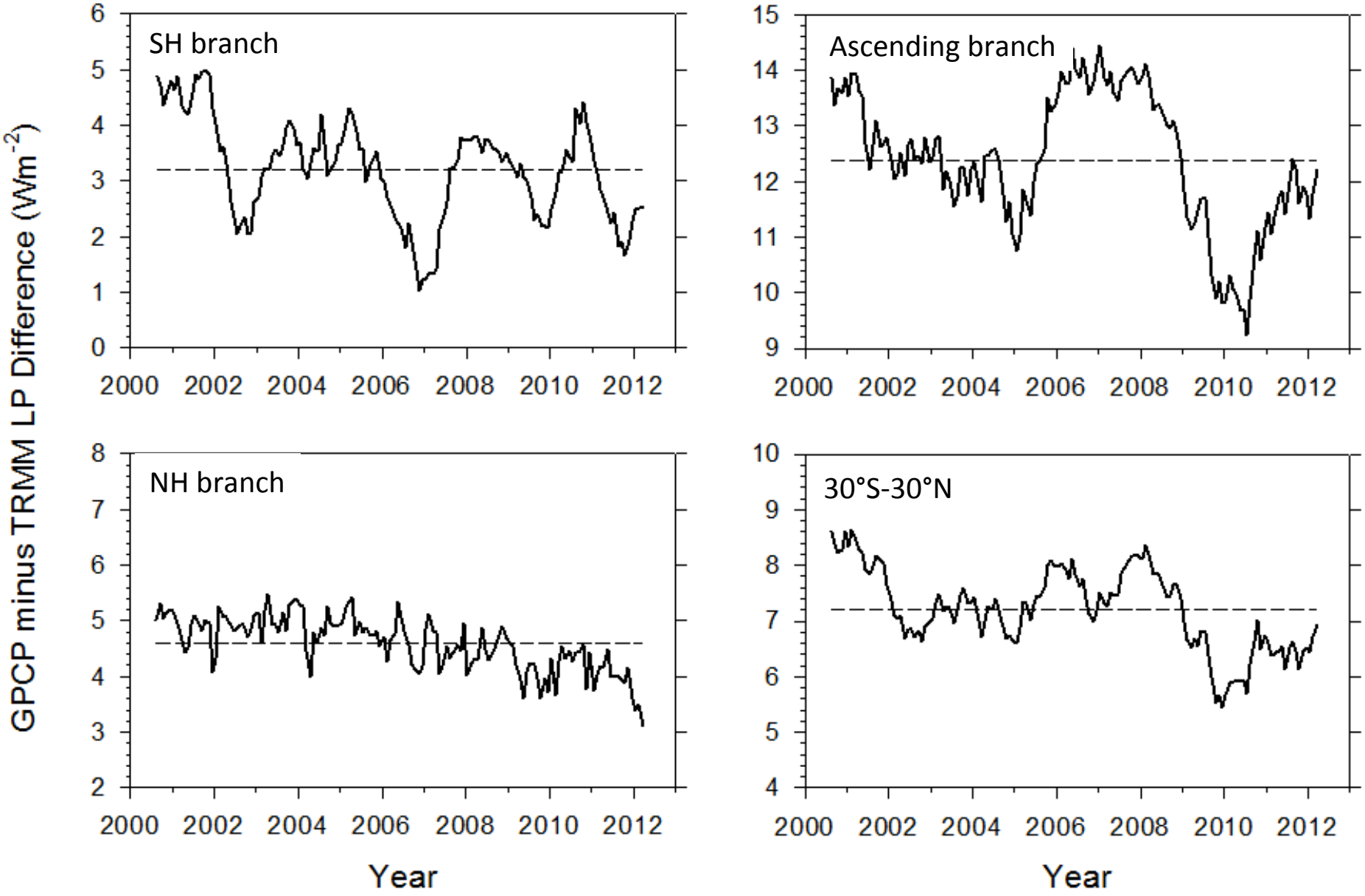

Average (Stdev) in LP for GPCP V2.2, TRMM (3A12), TRMM (3B43) (March 2000-Sept 2012)

	SH	Asc	NH	30ºS-30ºN
GPCP V2.2	59.6 (1.7)	132.8 (3.5)	51.1 (1.1)	88.4 (0.92)
TRMM_3A12	56.4 (1.2)	120.4 (0.73)	46.5 (0.73)	81.2 (0.73)
TRMM_3B43	57.1 (2.2)	142.4 (2.3)	52.5 (1.7)	93.3 (1.3)

The three data products agree to:

- 3 Wm^{-2} (5%) in the SH descending branch
- 6 Wm^{-2} (12%) in the NH descending branch
- **22 Wm^{-2} (17%) in the ascending branch**
- 12 Wm^{-2} (14%) for 30°S-30°N

Monthly Anomalies in Downward Surface Flux from CERES EBAF & Surface Observations (Approx. 30 Land and 19 Ocean sites)

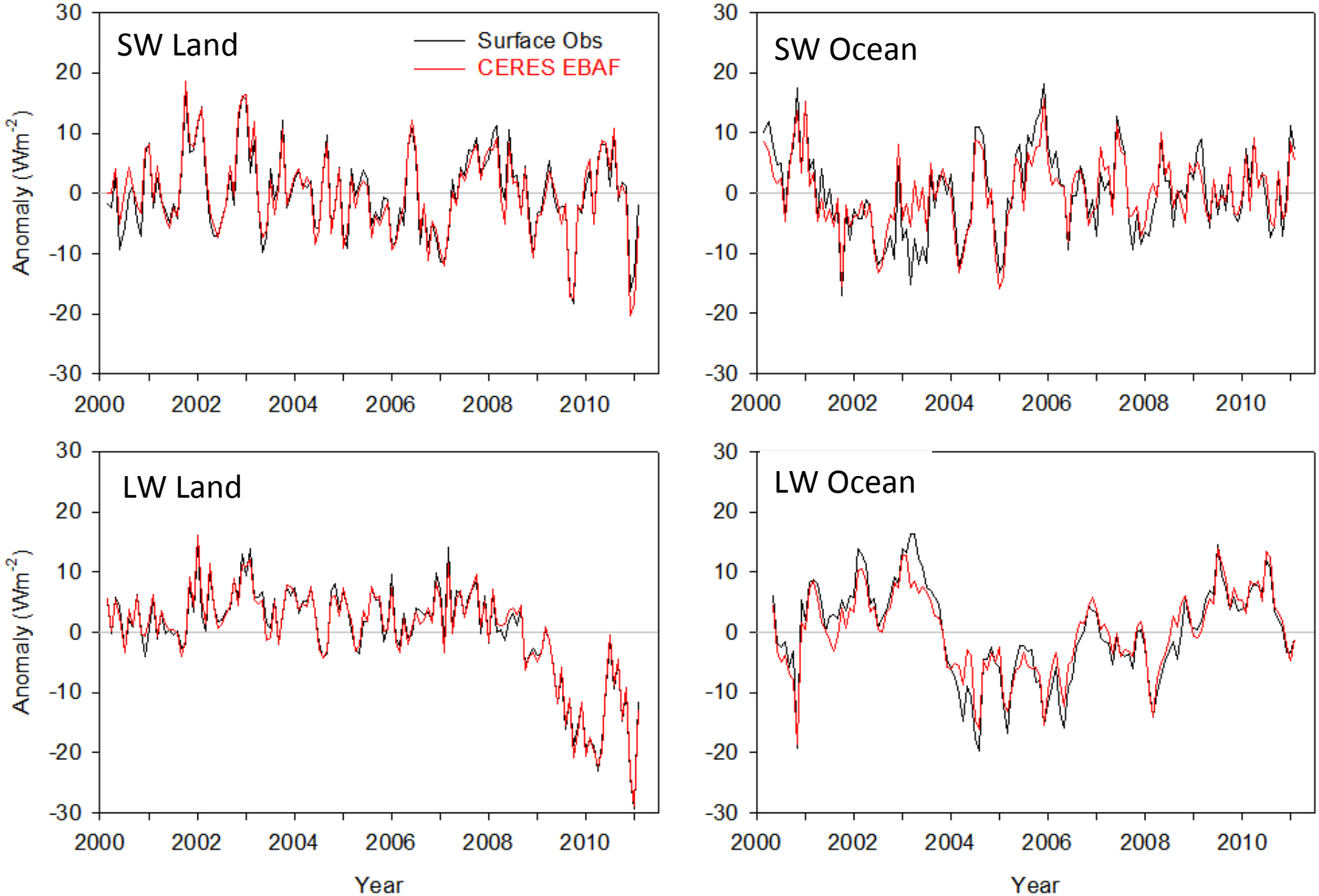

CERES EBAF Downward Surface Flux Comparison with Surface Observations

	SW Land					
	Mean (Wm^{-2})	σ(Mean) (Wm^{-2})	$\sigma(\delta)$ (Wm^{-2})	$\sigma(\delta_C-\delta_O)$ (Wm^{-2})	r	<N>
Surface Obs	180.8	30.1	6.8	1.8	0.97	29.2
CERES EBAF	180.1	29.2	7.0			
	LW Land					
	Mean (Wm^{-2})	σ(Mean) (Wm^{-2})	$\sigma(\delta)$ (Wm^{-2})	$\sigma(\delta_C-\delta_O)$ (Wm^{-2})	r	<N>
Surface Obs	315.1	25.6	8.0	1.1	0.99	29.5
CERES EBAF	315.8	27.0	8.0			
	SW Ocean					
	Mean (Wm^{-2})	σ(Mean) (Wm^{-2})	$\sigma(\delta)$ (Wm^{-2})	$\sigma(\delta_C-\delta_O)$ (Wm^{-2})	r	<N>
Surface Obs	236.0	11.8	7.1	3.1	0.9	17.5
CERES EBAF	240.0	11.3	6.1			
	LW Ocean					
	Mean (Wm^{-2})	σ(Mean) (Wm^{-2})	$\sigma(\delta)$ (Wm^{-2})	$\sigma(\delta_C-\delta_O)$ (Wm^{-2})	r	<N>
Surface Obs	400.1	8.1	7.8	2.7	0.95	5.4
CERES EBAF	398.7	7.0	6.7			

- CERES EBAF surface fluxes are well within uncertainty of surface observations (~ 5 Wm^{-2})

Interannual Anomalies in H: From Diabatic Heating vs Directly Calculations

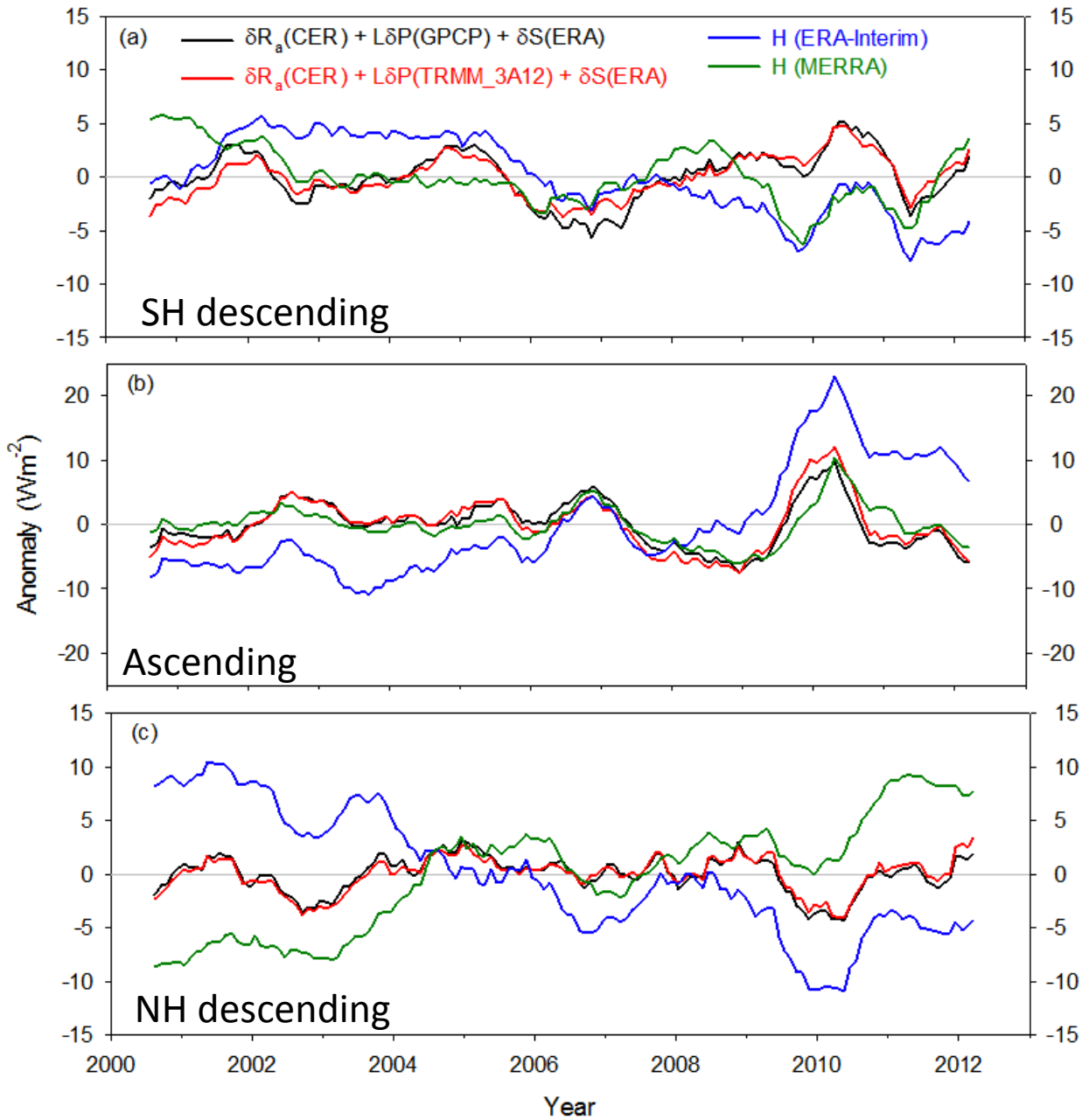

Relationship Between H and Mid-Tropospheric Vertical Velocity

- In the zonal mean, the vertical advective component dominates (Muller and O'Gorman, 2011), so that changes in the divergence of energy transport depend upon changes in mean vertical velocity, mean dry static stability, and their covariance:

$$\delta\left[\int\left(\omega\frac{\partial s}{\partial p}\right)\frac{dp}{g}\right]=\int\left(\delta[\omega]\frac{\partial s}{\partial p}\right)\frac{dp}{g}+\int\left(\omega\,\delta\left[\frac{\partial s}{\partial p}\right]\right)\frac{dp}{g}+\int\left(\delta[\omega]\delta\left[\frac{\partial s}{\partial p}\right]\right)\frac{dp}{g}$$

"Dynamic Component"

"Thermodynamic Component"

Interannual Anomalies in H and ω

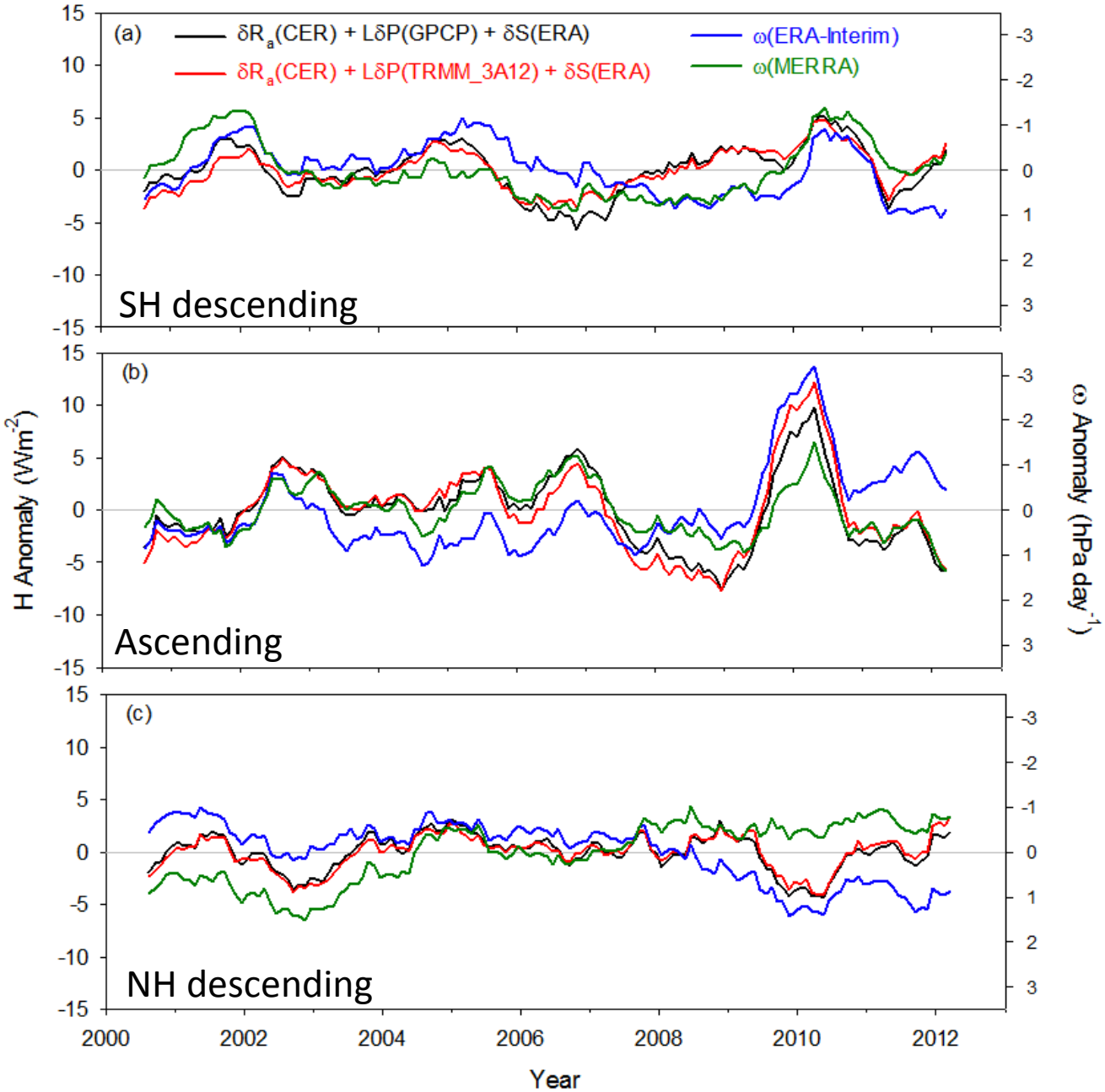

Summary

- Hadley circulation boundaries inferred from ERA-Interim stream function analysis follow seasonal migration in CERES LW CRE extrema in tropics.

- The latitudinal distance between southern and northern hemisphere LW CRE subtropical minima is correlated with ENSO index (MEI).

  -> Expansion during La Niña and contraction during El Niño.

- We find a -14 Wm^{-2} imbalance in the global mean atmospheric energy budget, suggesting that either global radiative cooling is overestimated and/or latent and/or sensible heating are underestimated.

  -> Differences amongst precipitation datasets largest in ascending branch, where precipitation is strongest.

  -> EBAF Surface fluxes within uncertainty of surface measurements.

- Interannual variation in atmospheric diabatic heating appears robust.
  - -> Implied divergence of DSE tracks with vertical velocity, while direct calculations from reanalyses show large drifts.
  - -> Stronger HC during El Niño, weaker HC strength during La Niña.

- Continued monitoring by stable satellite observations critical for understanding longer-term changes in atmospheric circulation & energy/water cycle.